JCTC Journal of Chemical Theory and Computation

ARTICLE

pubs.acs.org/JCTC

Characterization of the Ligand Receptor Encounter Complex and Its Potential for in Silico Kinetics-Based Drug Development

Karim M. ElSawy,[*,†,‡] Reidun Twarock,[†,‡,§] David P. Lane,[∥] Chandra S. Verma,[⊥] and Leo S. D. Caves[†,‡]

[†]York Centre for Complex Systems Analysis (YCCSA), [‡]Department of Biology, and [§]Department of Mathematics, University of York, York YO10 5YW, United Kingdom

[∥]P53 Laboratory (p53Lab, A* STAR), 8A Biomedical Grove 06−06, Immunos, Singapore 138648

[⊥]Bioinformatics Institute (A*STAR), 30 Biopolis Str., 07−01 Matrix, Singapore 138671

Supporting Information

ABSTRACT: The study of drug-receptor interactions has largely been framed in terms of the equilibrium thermodynamic binding affinity, an *in vitro* measure of the stability of the drug-receptor complex that is commonly used as a proxy measure of *in vivo* biological activity. In response to the growing realization of the importance of binding kinetics to *in vivo* drug activity we present a computational methodology for the kinetic characterization of drug-receptor interactions in terms of the encounter complex. Using trajectory data from multiple Brownian dynamics simulations of ligand diffusion, we derive the spatial density of the ligand around the receptor and show how it can be quantitatively partitioned into different basins of attraction. Numerical integration of the ligand densities within the basins can be used to estimate the residence time of the ligand within these diffusive binding sites. Simulations of two structurally similar inhibitors of Hsp90 exhibit diffusive binding sites with similar spatial structure but with different ligand residence times. In contrast, a pair of structurally dissimilar inhibitors of MDM2, a peptide and a small molecule, exhibit spatially distinct basins of attraction around the receptor, which in turn reveal differences in ligand orientational order. Thus, our kinetic approach provides microscopic details of drug-receptor dynamics that provide novel insight into the observed differences in the thermodynamic binding affinities for the two inhibitors, such as the differences in the entropic contributions to binding. The characterization of the encounter complex, in terms of the structure, topology, and dynamics of diffusive binding sites, offers a new perspective on ligand−receptor interactions and the potential for greater insight into drug action. The method, which requires no prior knowledge of the bound state, is a first step toward the incorporation of ligand kinetics into *in silico* drug development protocols.

INTRODUCTION

The *status quo* of drug development is the selective and optimal targeting of low-molecular-weight compounds to a particular bioactive molecule.[1] In general, this is carried out by *in vitro* optimization of the drug-target association constant (K_a), free energy of association (ΔG_a), or the half-maximal inhibitory concentration (IC_{50}). In this context, these parameters are used as quantitative measures (or proxies) of the drug biological activity.[2] This approach implicitly assumes closed-system conditions in which the target is exposed to an invariant concentration of the drug and thermodynamic equilibrium is assumed.[3] However, *in vivo* conditions are very different, as drug concentration is no longer invariant due to factors such as circulation, absorption, metabolism, and interaction with other cellular constituents. Under these conditions, it is becoming increasingly clear that the kinetics of drug binding, as measured by the association and dissociation rate constants (k_{on} and k_{off}) of drug target interactions, are of significant relevance to its biological activity.[1,4]

Initial work in developing quantitative structure−property relationships (QSPR) based on binding kinetics has confirmed the utility of both k_{on} and k_{off} as important and distinct factors relating to pharmacological and pharmacokinetic properties.[5] It has been observed that, in lead optimization, a decrease in the association constant (K_d) often results in a lowering of k_{off} by proxy, due to the typically smaller dynamic range of k_{on}. Unlike k_{off}, k_{on} is usually diffusion-controlled and hence not amenable to optimization. Indeed, increasing k_{off} was found to be strongly related to HIV-1 protease resistance to the inhibitor saguiavir.[6] This was further confirmed by a study of the kinetics of the interaction between drug-resistant variants of HIV-1 protease and several clinically used inhibitors (amprenavir, indinavir, nelfinavir, ritonavir, and saquinavir), where the reduction of affinity was related to a combination of decreased k_{on} and increased k_{off}.[7] Similarly, the development of resistance in EGFR has been associated with altered kinetics,[8] where p53 DNA site-specific recognition was found to rely more on differences in binding k_{off} rather than on differences in affinities.[9] These observations have led a number of recent researchers to stress a greater role for drug binding kinetics in therapeutic differentiation strategies,[10] mitigating off-target mediated toxicity and leading to improved drug safety and tolerability.[4] It is becoming clear that the off-rate k_{off} or the drug-target residence time τ ($\tau \sim 1/k_{off}$) is an important and perhaps crucial property for drug lead optimization,[1,4,11−13] thereby providing an alternative route to improving the therapeutic utility of a drug.[10]

Received: August 11, 2011
Published: December 28, 2011

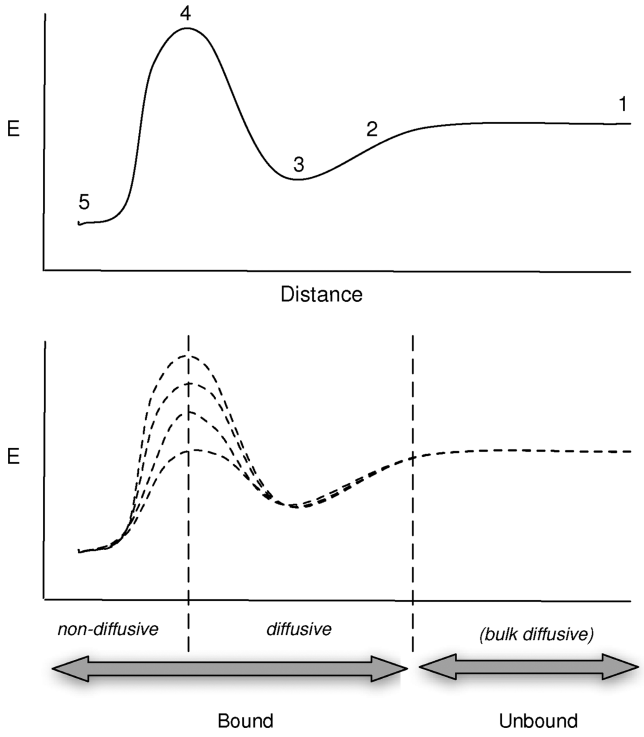

Figure 1. (Upper) Traditional view of the free energy profile along the reaction coordinate of ligand−receptor interaction. Different domains of interaction are schematically depicted: (1) free diffusion, (2) electrostatic steering, (3) encounter complex, (4) energy barrier crossing, and (5) formation of the bound (final) complex. (Lower) An alternative view with two broad regimes of interaction: unbound (free bulk diffusion) and bound, which incorporates both the restricted diffusion of the encounter complex and the nondiffusive characteristics of (final) bound states. In the general case, due to ligand and receptor conformational flexibility, the energy surface is dynamic—and with the variation in 4 shown for illustration. Under nonequilibrium conditions, both the occupation of states and the barrier height are time-dependent.

We consider key stages of ligand−receptor interactions via an illustrative reaction coordinate (Figure 1). In this scheme, the traditional focus is on the energy barrier (labeled 4) separating the freely diffusing ligand (labeled 1) from the bound complex (labeled 5). At equilibrium, this barrier can be related to the association and dissociation rates (k_{on} and k_{off}). However, prior to reaching equilibrium, an encounter complex is formed. The encounter complex corresponds to the configuration of the ligand receptor complex prior to crossing the energy barrier to the final bound state. The process of ligand−receptor interaction can, therefore, be described in terms of three distinct regimes: *unbound* (in bulk solution), *nondiffusively bound* (the classic binding site, and the focus of the thermodynamic approach to drug interaction), and an intermediate *diffusively bound* regime characterized by the *encounter complex* (Figure 1). The ligand in this diffusively bound regime is spatially restrained in the vicinity of the receptor due to net associative influx.

The encounter complex is therefore a prerequisite for the binding reaction to proceed and is differentiated from other configurations by the requirement that *the ligand association rate is much higher than its dissociation rate*.[14] The residency of the encounter complex increases the possibility of mutual perturbation of the ligand and the receptor conformational landscape, which may lead to a reduction of the barrier height. This is consistent with the observation that the forward rate constant k_{on} is diffusion-limited in a large number of biological processes.[15−17]

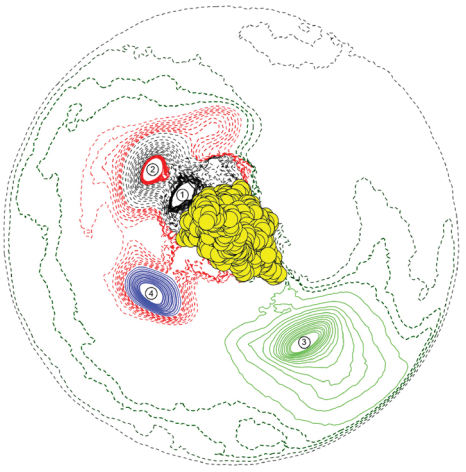

Figure 2. A 2D illustration of the partitioning of the space around the MDM2 receptor (yellow) into four different basins of attraction (shown as solid lines) and their connecting superbasins (shown as dashed lines). The basins of attraction correspond to regions of space where the rate of association of the ligand−receptor encounters is higher than the rate of dissociation−formation of the ligand−receptor encounter complex. This is ensured by two constraints: (1) the inward direction of the gradient of the ligand density contours in these regions (i.e., inward overall ligand influx) and (2) the requirement that the contours be closed such that the ligand motion in these region is spatially restricted. Hot spots within these basins are labeled in ascending order according to the corresponding ligand residence time.

Amidst the flux and clearance that is characteristic of the *in vivo* situation, the encounter complex represents a higher local availability (or "concentration") of the drug around the target. This sustains the influence of the drug on the target (i.e., perturbation of receptor conformational states, via conformational selection, or induced fit), which in turn is responsible for the biological response.[1] Thus, the residence time of the encounter complex emerges as an important, and as yet underexplored, kinetic factor in ligand−receptor interactions in a pharmacological context.

Currently, myriad computational tools exist to support drug development within the thermodynamic approach.[18−21] More recently, steered molecular dynamics simulations have enabled the successful discrimination of good and bad binders among a set of molecules to a receptor, thus pointing toward the relevance of k_{off}.[22] In addition, with the availability of computers that enable much longer simulation times, atomistic simulations have revealed the pathways of drug binding to receptors and have displayed apparent kinetics that are close to the experimentally determined ones.[23,24] However, both of these methods require very long simulations that are currently not generally accessible, which in turn make them not amenable to easy statistical analyses. Moreover, they do not provide a general framework for addressing the kinetics of ligand protein interactions.

Here, we introduce a novel method to compute kinetic information related to drug-target interactions that could be a powerful and complementary addition to the drug development toolkit.[25] We describe a computational strategy for the characterization of the ligand−receptor *encounter complex*. On the basis of the definition introduced above, we regard the encounter complex as being in terms of *basins of attraction* of the ligand

around the receptor, and we provide a method for their identification. We estimate the residence time in these basins of attraction by integration of the ligand spatial probability density derived from multiple ligand trajectories in Brownian dynamics simulations.

The use of a clear physical criterion in defining the encounter complex allows for a blind (i.e., unbiased) characterization of multiple basins of attraction representing kinetically distinct diffusively bound states with their own characteristic residence times (Figure 2). This framework offers the possibility of significantly supplementing the current models of drug-receptor interactions with quantitative parameters relating to the structure (spatial distributions of the drug within the basins of attraction), topology (connectivity of the basins), and dynamics (flux in, out, and between basins) within the diffusive-bound regime.

MATERIAL AND METHODS

Diffusional Dynamics of Ligand Receptor Interaction. Brownian dynamics (BD) simulations of the ligand protein diffusional encounters were carried out for the association schemes 1 and 2 using the SDA package.[26,27]

$$\begin{array}{l} \quad (protein) \quad (ligand)\ (complex) \\ HSP90+\begin{cases} ver\text{-}49009 \rightarrow HSP90 : ver\text{-}49009 \\ ver\text{-}50589 \rightarrow HSP90 : ver\text{-}50589 \end{cases} \end{array} \quad (1)$$

$$\begin{array}{l} \quad (protein)\ (ligand) \quad (complex) \\ MDM2+\begin{cases} \text{p53} \rightarrow \text{MDM2 : p53} \\ \text{nutlin} \rightarrow \text{MDM2 : Nutlin} \end{cases} \end{array} \quad (2)$$

Brownian Dynamics Setup. The BD trajectories were propagated by solving the translational and rotational diffusion equations, using the Ermak−McCammon algorithm[28] as implemented in the SDA package version 4.23b. The diffusion coefficients were calculated using the HYDROPRO software.[29] Initially, the center of mass (COM) of the protein was placed at the origin, and the ligand was placed at a b = 150.0 Å COM−COM separation relative to the protein center of mass. At this separation, there is no preferential orientation of the ligand since the electrostatic potential of the protein is nearly isotropic at distances greater than 80 Å from its center of mass. A time step of 0.1 ps was used when the COM−COM separation was less than 90 Å. At larger separations, the time step was increased linearly with a slope of 0.5 ps Å^{-1}. The simulations were terminated if the ligand−protein COM−COM separation exceeded $c = 3b$ Å.

In scheme 1, multiple conformations of the VER-49009 and VER-50589 ligands were used as initial structures for BD simulation of the ligand diffusion around the HSP90 protein (PDB ID: 2uwd). The ligand conformations were selected on the basis of principal component analysis (PCA) of constant-temperature MD trajectories (1 ns) of the unbound ligand using the Merck force field within CHARMM. The selected ligand conformations correspond to high-density regions in the ligand conformational landscape as revealed by PCA. In scheme 2, 15 snapshots of the ligand protein conformations were extracted from equilibrated MD trajectories of the p53 peptide (ETFSDLWKLLPEN) and nutlin-2 MDM2 bound complexes.[30] In both schemes, a large number of BD trajectories (100 000 and 750 000 for schemes 1 and 2, respectively) were generated and checked for convergence with respect to the total residence time of the ligand around the receptor (see below). Typically, 50 000 BD trajectories were found to be sufficient to reach convergence in both schemes.

In the BD simulations, the forces between the ligand and the protein derive from steric, desolvation, and electrostatic interactions. Steric interactions were accounted for implicitly through the use of steric exclusion grids (grid spacing of 1 Å) centered on both protein and ligand. The electrostatic force on any atom of the ligand was calculated by multiplying its charge by the electrostatic potential of the protein at that spatial position. The electrostatic potential around the protein and ligand was calculated by numerically solving the nonlinear Poisson−Boltzmann equation[31,32] on a grid with dimensions of 161 × 161 × 161 Å centered at the ligand/protein using the APBS program.[33] Using a grid spacing of 1 Å (as required by the SDA package) results in computational efficiencies in the BD simulations. Adapted PEOE atomic charges and radii of the ligand and the protein atoms were assigned using the PDB2PQR program.[34,35] The solvent dielectric constant was set to 78.5 and the protein interior dielectric constant to 4; the salt concentration was set to 0.15 M. The solute−solvent boundary was defined at the van der Waals surface because molecular surface definition was found to result in significant underestimation of the association rates in some cases.[36] During the BD simulations, for the sake of computational efficiency, the full set of atomic charges of the ligand was replaced by a smaller set of effective charges that accurately reproduced their calculated electrostatic potential.[37] The effective charges were derived by the ECM module in the SDA package so as to reproduce the electrostatic potential at the accessible surface (defined by a probe of 4 Å) in a 3-Å-thick layer extending outward from each structure.

Desolvation effects were incorporated through a desolvation penalty grid[38] around the ligand and the protein using a scaling factor of 1.67, consistent with the surface definition for the solute−solvent boundary.[36] Use of explicit water has been shown in a number of studies to be an important factor in molecular association[39,40] and the formation of the ligand-bound complex[41] (labeled 5; Figure 1). However, since we focus on the encounter complex (labeled 3; Figure 1), outside its conventional binding site, we believe, an implicit account of desolvation effects using a penalty grid is a reasonable choice consistent with the use of BD simulations.

Convergence of the BD Simulation. In order to check for convergence of the BD simulations, the total residence time of the ligand around the protein was estimated by aggregating successively larger numbers of BD trajectories in post processing. The total residence time of the ligand was then computed via integration of the residence time radial profile. Since the BD trajectories are independent, there is no particular order in which to aggregate the data. To provide a robust estimate of convergence, the following procedure was used. The BD trajectories were split randomly into bins that comprise 5000 trajectories each; the bins were then sampled without replacement and spliced randomly to form bigger bins that comprise 10 000, 15 000, 20 000, etc. trajectories. The process was repeated 1000 times, and the average residence time of the ligand around the protein was then computed for each bin (Supporting Information, Figure 1). The BD simulations were found to converge beyond 50 000 trajectories for both schemes 1 and 2.

Kinetics-Based Approach for the Identification of Encounter Complex Basins of Attraction. The following algorithm forms the basis of our kinetics-based approach to identifying the dynamically derived ligand spatial density around the receptor and partitioning it into distinct basins of attraction, which comprise

the ligand−receptor encounter complex. From the trajectory data, a 3D spatial probability density grid is constructed around the receptor by computing the average frequency of the ligand center of mass visiting individual spatial grid cells. The grid dimensions were chosen so as to extend 200 Å in each direction with a grid spacing of 1 A. The root-mean-square displacement of the center of mass of the ligand during the BD simulations (∼0.15 Å in schemes 1 and 2) sets a lower limit for the grid spacing that can be used. The choice of a grid spacing of 1 Å reflects a balance between retaining dynamical information and tractable spatial resolution: in practice, it generates a detailed and smooth spatial probability density landscape.

The 3D ligand spatial density grid is contoured at equally spaced contour intervals that extend from the highest density (strongly interacting with the receptor: diffusely bound regime) to the lowest density (weak/noninteracting: diffusive regime). Closed contours at the highest level of density represent interaction "hot spots". Closed contour surfaces at successively lower density levels that encompass each individual hot spot are then accumulated. As a consequence of following the density gradient in this manner, the ligand flux in these regions is such that the average rate of inward ligand association (i.e., toward the hot spot) is higher than its average outward dissociation rate. As the contour surfaces are "closed", the process therefore ensures that the direction of the ligand density gradient is maintained inward from all directions. These characteristics, which result from restriction (or channelling) of the ligand motion in the diffusional trajectories, result in these regions acting as basins of attraction. The connectivity between different basins of attraction is determined by detecting closed contour surfaces that encompass multiple hot spots: such regions represent superbasins of attraction within a global disconnectivity tree.[42]

This scheme, based on ligand−receptor binding dynamics, yields a partitioning of the ligand spatial density around the receptor into kinetically distinct, spatially resolved encounter complex basins of attraction that correspond to putative binding sites in the diffusively bound regime. The identification of these sites does not require prior knowledge of a (conventional nondiffusive) binding site on the receptor, or the use of other *ad hoc* criteria.[14,27,43] This is notable, in view of the increasing importance of the role of allosteric sites in modulating activity[44] which are difficult to infer from static methods such as X-ray crystallography.

Estimation of Ligand Site-Specific Residence Time (τ_{LR}). The ligand *site-specific residence time* is computed for individual basins of attraction by numerical integration of the time-averaged ligand probability density in each basin of attraction. Using small contour intervals, in which the ligand density D is effectively constant, the integral can be approximated by

$$\tau_{LR} = \sum_{n=2}^{N} \Delta t(V_n - V_{n-1})(D_n + D_{n-1})/2$$

where $(V_n - V_{n-1})$ is the volume enclosed between two consecutive contour surfaces at ligand densities D_n and D_{n-1} and Δt is the time step used in the BD simulation. In the case of multiple basins of attraction, it may be convenient to express the *fractional residence time* of a given basin as a proportion of the total residence time over all basins.

RESULTS AND DISCUSSION

In order to illustrate the applicability of our approach, we considered two ligand−receptor systems: (1) interactions of two structurally homologous inhibitors (VER-50589 and VER-49009) with their target Hsp90 and (2) interactions of two very different ligands, an α-helical peptide mimic of p53 and a nonpeptide ligand (Nutlin), with MDM2, the negative regulator of p53.

1. Hsp90−Inhibitor Interactions. Hsp90 inhibitors cause the inactivation and eventual degradation of Hsp90 client proteins and have shown promising antitumor activity in preclinical model systems.[45] However, the relationship between the biological activity and thermodynamic characteristics of a number of these inhibitors remains unclear.[46] Recently, a potent isoxazole analogue of 3,4-diarylpyrazole resorcinols, called VER-50589, has been identified. This compound is 9-fold more potent than a highly homologous analogue, the pyrazole VER-49009.[46] Interestingly, the key difference between the two compounds is the introduction of an amine (N−H) group (and thus a new H-bond donor) into a heterocyclic ring, resulting from the replacement of an oxygen atom in VER-50589 by a nitrogen atom in VER-49009 (see Figure 3a, top).

The crystal structures of these inhibitors bound to the N-terminal domain of the Hsp90 monomer reveal a "virtually identical binding mode";[46] calorimetric analysis revealed a tigher binding for VER-50589 vs VER-49009 (K_d: 4.5 vs 78.0 nmol L^{-1}) attributed to a higher enthalpy of VER-50589 binding, yet the rationale for this remains unclear.[46] However, a kinetic analysis of ligand binding has suggested that the higher cellular activity of VER-50589 relative to VER-49009 may be associated with an approximately 10-fold slower off-rate for VER-50589 compared to VER-49009, leading to higher cellular concentrations.[47]

BD simulations (Figure 3) reveal that both inhibitors exhibit very similar encounter complex distributions around the Hsp90 protein (Figure 3b) forming three main basins of attraction in proximity to the residues Thr:65, Gly:125, and Glu:205 on the receptor surface (VER-50589 exhibits a very minor fourth basin). A comparison of the fractional residence times of the ligands within these basins shows two distinct patterns: VER-49009 exhibits an essentially equal distribution of the ligand across the three basins (fractional residence times of ∼35, 35, and 29%), whereas VER-50589 preferentially occupies a single basin (fractional residence times of 50, 33.5, 14%). The unequal occupancy within the three basins leads to differences in the effective local concentration of the ligand.

Although we cannot draw firm conclusions from these preliminary results, we can begin to illustrate how this new picture of drug-target interactions could provide additional insight into the mechanism of drug action. Without consideration of major allosteric effects, a working assumption is that the degree of influence that a ligand has on the receptor is proportional to the amount of time it is available to exert that influence. In this context, the encounter complex basin residence time profile of VER-49009 suggests a higher degree of ligand depletion than VER-50589. By contrast, VER-50589 spends more time residing in a localized region close to the receptor. Such characteristics are of interest in relation to the superior pharmacodynamics (longer duration of action) and enhanced antitumor efficacy of VER-50589 vs VER-49009 *in vivo*[46] and may offer new perspectives on future drug development.

2. MDM2−Inhibitor Interactions. The protein p53 protects cells from various sorts of damage, and its levels are controlled in a negative feedback loop with the ligase MDM2.[48] This interaction is critical for therapeutic intervention in tumors that have overexpressed MDM2, leading to an intense search for MDM2 inhibitors.[49,50] There are two major avenues being explored for

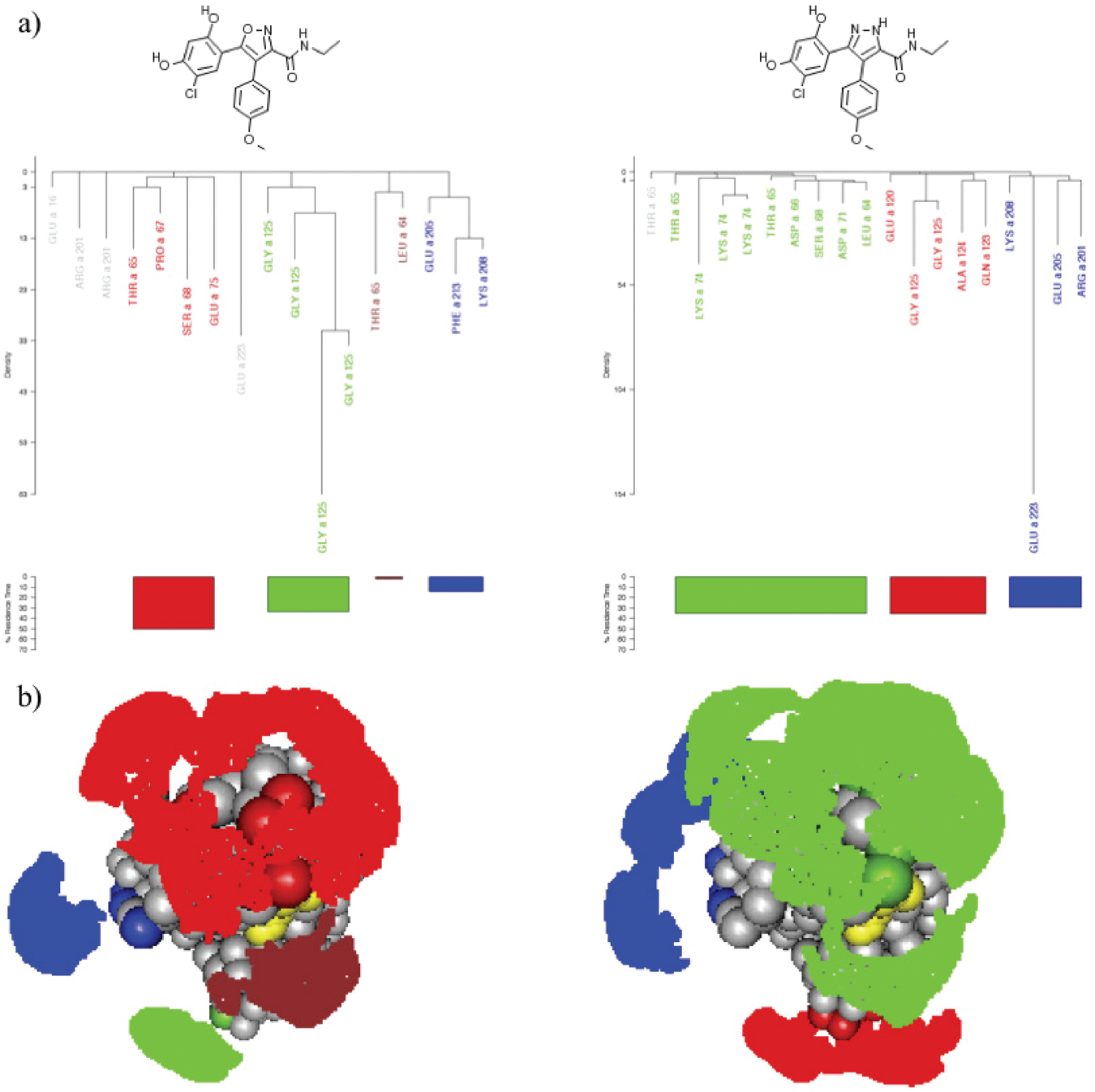

Figure 3. (a) The disconnectivity trees of the density of the ligand−Hsp90 encounter complex and the corresponding fractional residence times of the different basins of attaction of VER-50589 (left) and VER-49009 (right) upon interaction with the Hsp90 N-terminal domain. The leaves of the disconnectivity tree correspond to different basins of attraction; sets of connected basins form superbasins that are shown in different colors such that those corresponding to the superpbasin with the highest residence time are shown in red. The distribution of the center of mass of the ligand within these superbasins around the Hsp90 is shown in b using the same color scheme. Residues closest to the basins within each superbasin are labeled accordingly in a and b. The ligand within the active site as determined by X-ray crystallography (PDB ID: 2uwd) is shown in yellow for each case.

inhibitors: small molecules (e.g., Nutlins) and peptide mimics of p53, both of which disrupt or prevent p53−MDM2 intercations; indeed some are now entering clinical trials. However, in general, the peptidic inhibitors have not been as effective as Nutlins,[51] a trend that is in line with their relative thermodynamic binding affinity.[52] Here, we apply our methodology to examine how binding kinetics relate to these observed differences in activity. In contrast to the Hsp90 inhibitors, the distribution of the basins of attraction of Nutlin and the α-helical peptide around MDM2 are distinctly different (Figure 4a). This reveals that the characteristics of interactions with a given receptor (and thus potentially the mechanism of action) can vary between ligands. This is important, as when developing potential inhibitors, such as nutlins and peptidomimetics, ligand optimization is currently carried out in terms of thermodynamic parameters, assuming a largely invariant binding site and thus similar modes of interactions. In contrast,

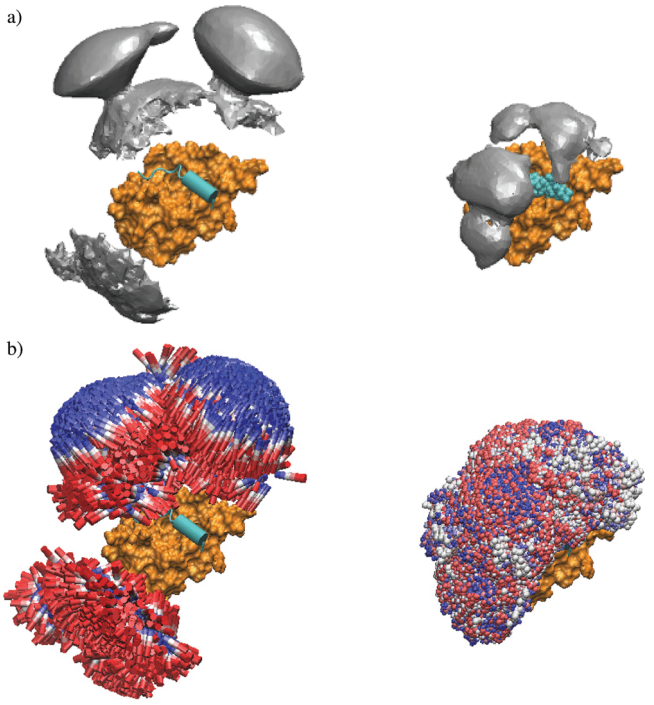

Figure 4. (a) The basins of attraction (gray) of the α-helical peptide ligand (left) and Nutlin-2 (right) upon interaction with the MDM2 (orange). The final bound complex is shown in cyan in cartoon and VDW representations. The corresponding structures of the encounter complex within each basin are shown in b. In order to illustrate the direction of the molecular structures within these basins, the structures are colored according to the atom index of each of them using a color palette that changes smoothly from blue (first atom) to red (last atom).

the kinetic profiles, in terms of encounter complex basins of attraction, suggest that this assumption needs to be re-examined. In agreement with the discovery of the importance of allosteric interactions in peptide-MDM2 interactions,[30] the spatial ditribution of the basins of attraction of the α-helical peptide suggests that the initial diffusive encounter between the peptide and MDM2 takes place far from the (classic nondiffusive) binding site, at the N- and C-termini of MDM2 (Figure 4a, left). Moreover, within the basins of attraction, the distribution of ligand configurations exhibits a relatively high degree of order in terms of helix orientation (Figure 4b, left). This reflects the significant degree of loss of rotational entropy upon peptide interaction with the MDM2 that has to be compensated for by enthalpic interactions upon formation of the final bound complex.[52] The orientational order of the peptides clearly stems from alignment of the ligand helix dipole moment with the electrostatic potential of the MDM2 receptor. Interestingly, the peptide helix orientation with respect to the receptor surface is reversed within the two basins. By comparison, interaction of Nutlin with MDM2 takes place via two basins of attraction that directly interact with the clefts of the (classic nondiffusive) binding site on the MDM2 surface (Figure 4a, right). By contrast, the distribution of structures of the Nutlin encounter complex within these basins does not exhibit the same degree of order as observed for the peptide inhibitor (Figure 4b, right), suggesting that as a consequence of the orientational preordering, the entropic loss upon Nutlin binding to MDM2 will be smaller than the peptide, thus contributing to its higher affinity.

This new kinetics-based mechanistic insight complements the traditional thermodynamic approach to drug optimization, which focuses attention on the (nondiffusive) bound state, which necessarily has a more restricted configurational distribution than diffusively bound encounter complex states. In the thermodynamic approach, optimization (in terms binding affinity) of peptidic ligands would be based on maximizing the enthalpic contribution to binding in order to compensate for the entropic loss on moving from the (bulk diffusive) unbound regime. From our kinetics-based analysis of the encounter complex structural distribution, we see the role of the helix dipole in restricting the orientational freedom of the peptide ligand, compared to Nutlin. This observation could provide new avenues for exploitation in drug optimization, for example, to tune binding properties by engineering peptidic ligand dipole moments to modify the configurational ordering in the encounter complex—a new approach that emerges from our methodology.

CONCLUSIONS

We present an effective and principled computational approach for the kinetic characteristisation of ligand−receptor interactions with a focus on the encounter complex, defined clearly as states where the ligand−receptor association rate is higher than the dissociation rate. Our approach to identifying these diffusive binding sites does not rely upon the assumption of reaching thermodynamic equilibrium or on prior knowledge of the bound state. Instead, we adopt a dynamical approach: generating trajectories representing ligand−receptor diffusional encounters on a natural time scale (subject to certain technical constraints), representing the time for the ligand to diffusionally engage and subsequently disengage from the receptor. Using data from multiple trajectories, we derive spatial densities of the ligand around the receptor. The ligand spatial distribution can then be partitioned into distinct basins of attraction, representing diffusive binding sites. Residence times within these sites are estimated by numerical integration of the corresponding ligand denisites. We emphasize that the residence times estimated in this procedure relate to the encounter complex and do not incorporate contributions arising from the classic bound state, which is the subject of ongoing work.

The importance of the residence time in shaping the biological activity of drug candidates has been the focus of several recent studies.[1,3,4,12] Thus, a quantiative structural and kinetic characterization of diffusively bound ligand−receptor interactions provides additional information that may provide greater (or at least complementary) insight into the "mechanism" of drug action *in vivo* than that provided by traditional thermodynamic approaches. Specifically, the introduction of a new set of microstates (encounter complex basins of attraction) opens up new avenues for gaining a greater understanding of the relationship of the microscopic ligand−receptor dynamics to the effective macrostates that underpin thermodynamic treatments of the binding process.

We have applied the methodology to two different systems: Hsp90 inhibitors and MDM2 inhibitors. For Hsp90, we found that the redistribution of the ligand residence time across the different basins of attraction is likely to be an important factor in shaping the biological activity of structurally related inhibitors. For MDM2, on the other hand, we showed that structurally unrelated inhibitors, an α-helical peptide and Nutlin, exhibit two distinctly different patterns of interaction with the MDM2 receptor. The basins of attraction of the α-helical peptide around MDM2 are located far from the ligand binding site, suggestive of

an allosteric mechanism, while the locations of the basins for Nutlin are indicative of more direct interactions with the classic ligand binding site. In our study, the peptide conformation is restricted to be largely α-helical. This is justified by reference to the increasing use of "stapled" peptides as therapeutic agents which rely on stabilizing the peptide intro an α-helical conformation through the use of a hydrocarbon bridge.[53−55] The introduction of the bridge does not significantly affect the electrostatic potential of the peptide, and therefore we anticipate that its absence in our model will not significantly affect our results since electrostatic interaction is the main driving force for the formation of the encounter complex.

In this proof of principle study, we employ multiple static conformations of the ligand and receptor and thus cannot address cooperative features of molecular recognition such as induced fit of receptor−ligand conformational states.[56] However, such effects can be incorporated into the approach, albeit at additional computational cost, by the use of nested BD/MD simulations, which are the subject of ongoing study.

The methodology is timely given the growing realization of the importance of drug binding kinetics, particularly the drug-target residence time, for optimizing drug efficacy *in vivo*. The additional insight provided by this kinetics-based characterization could provide a powerful complement to the traditional structure-based computational drug optimization techniques that are largely focused on the thermodynamics of drug−receptor interactions in the classic (nondiffusive) binding site. Of particular promise is the potential for additional insight into the mechanisms of drug action afforded by a richer picture of molecular interactions with the adoption of a complex dynamical (or even adaptive) systems framework (e.g., trajectories, basins of attraction), over traditional equilibrium thinking (e.g., states, static distributions). We offer this approach as an example of a new breed of computational tools to explore the new paradigm of kinetic-based drug development.

■ ASSOCIATED CONTENT

Supporting Information. Convergence of the residence time as a function of the number of BD trajectories. This material is available free of charge via the Internet at http://pubs.acs.org.

■ AUTHOR INFORMATION

Corresponding Author

*E-mail: karim.elsawy.email@gmail.com.

Notes

The authors declare no competing financial interest.

■ ACKNOWLEDGMENT

We thank Prof. Roderick E. Hubbard for many helpful discussions and for suggesting the Hsp90 test case. We are very grateful to Drs. Garib Murshudov and Seishi Shimizu for the provision of computing resources.

■ REFERENCES

(1) Copeland, R. A.; Pompliano, D. L.; Meek, T. D. Drug-target residence time and its implications for lead optimization. *Nat. Rev. Drug Discovery* **2006**, *5* (9), 730–739.

(2) Kenakin, T. Quantifying Biological Activity in Chemical Terms: A Pharmacology Primer to Describe Drug Effect. *ACS Chem. Biol.* **2009**, *4* (4), 249–260.

(3) Tummino, P. J.; Copeland, R. A. Residence time of receptor-ligand complexes and its effect on biological function. *Biochemistry* **2008**, *47* (20), 5481–92.

(4) Copeland, R. A. The dynamics of drug-target interactions: drug-target residence time and its impact on efficacy and safety. *Expert Opin. Drug Discovery* **2010**, *5* (4), 305–310.

(5) Andersson, K.; Hämäläinen, M. D. Replacing affinity with binding kinetics in QSAR studies resolves otherwise confounded effects. *J. Chemom.* **2006**, *20* (8−10), 370–375.

(6) Maschera, B.; Darby, G.; PalÃ°, G.; Wright, L. L.; Tisdale, M.; Myers, R.; Blair, E. D.; Furfine, E. S. Human Immunodeficiency Virus. Mutations in the viral protease that confer resistance to saquinavir increase the dissociation rate constant of the protease-saquinavir complex. *J. Biol. Chem.* **1996**, *271* (52), 33231–33235.

(7) Shuman, C. F.; Markgren, P. O.; Hamalainen, M.; Danielson, U. H. Elucidation of HIV-1 protease resistance by characterization of interaction kinetics between inhibitors and enzyme variants. *Antiviral Res.* **2003**, *58* (3), 235–42.

(8) Yun, C.-H.; Mengwasser, K. E.; Toms, A. V.; Woo, M. S.; Greulich, H.; Wong, K.-K.; Meyerson, M.; Eck, M. J. The T790M mutation in EGFR kinase causes drug resistance by increasing the affinity for ATP. *Proc. Natl. Acad. Sci. U.S.A.* **2008**, *105* (6), 2070–2075.

(9) Petty, T. J.; Emamzadah, S.; Costantino, L.; Petkova, I.; Stavridi, E. S.; Saven, J. G.; Vauthey, E.; Halazonetis, T. D. An induced fit mechanism regulates p53 DNA binding kinetics to confer sequence specificity. *EMBO J.* **2011**, *30* (11), 2167–2176.

(10) Swinney, D. C. Applications of Binding Kinetics to Drug Discovery: Translation of Binding Mechanisms to Clinically Differentiated Therapeutic Responses. *Pharm. Med.* **2008**, *22* (1), 23–34.

(11) Swinney, D. C. The role of binding kinetics in therapeutically useful drug action. *Curr. Opin. Drug Discovery Dev.* **2009**, *12* (1), 31–9.

(12) Zhang, R.; Monsma, F. The importance of drug-target residence time. *Curr. Opin. Drug Discovery Dev.* **2009**, *12* (4), 488–96.

(13) Lu, H.; Tonge, P. J. Drug-target residence time: critical information for lead optimization. *Curr. Opin. Chem. Biol.* **2010**, *14* (4), 467–74.

(14) Gabdoulline, R. R.; Wade, R. C. On the protein-protein diffusional encounter complex. *J. Mol. Recognit.* **1999**, *12* (4), 226–34.

(15) Tzafriri, A. R.; Levin, A. D.; Edelman, E. R. Diffusion-limited binding explains binary dose response for local arterial and tumour drug delivery. *Cell Proliferation* **2009**, *42* (3), 348–363.

(16) Raman, C. S.; Jemmerson, R.; Nall, B. T.; Allen, M. J. Diffusion-limited rates for monoclonal antibody binding to cytochrome c. *Biochemistry* **1992**, *31* (42), 10370–10379.

(17) McGahay, V. Inertial effects and diffusion. *J. Non-Cryst. Solids* **2004**, *349*, 234–241.

(18) Zoete, V.; Grosdidier, A.; Michielin, O. Docking, virtual high throughput screening and in silico fragment-based drug design. *J. Cell. Mol. Med.* **2009**, *13* (2), 238–248.

(19) Gilson, M. K.; Zhou, H. X. Calculation of protein-ligand binding affinities. *Annu. Rev. Biophys. Biomol. Struct.* **2007**, *36*, 21–42.

(20) Gilson, M. K.; Given, J. A.; Bush, B. L.; McCammon, J. A. The statistical-thermodynamic basis for computation of binding affinities: a critical review. *Biophys. J.* **1997**, *72* (3), 1047–1069.

(21) Durrant, J. D.; McCammon, J. A., Computer-aided drug-discovery techniques that account for receptor flexibility. *Curr. Opin. Pharmacol. 10*, (6), 770-774.

(22) Colizzi, F.; Perozzo, R.; Scapozza, L.; Recanatini, M.; Cavalli, A. Single-Molecule Pulling Simulations Can Discern Active from Inactive Enzyme Inhibitors. *J. Am. Chem. Soc.* **2010**, *132* (21), 7361–7371.

(23) Shan, Y.; Kim, E. T.; Eastwood, M. P.; Dror, R. O.; Seeliger, M. A.; Shaw, D. E. How Does a Drug Molecule Find Its Target Binding Site?. *J. Am. Chem. Soc.* **2011**, *133* (24), 9181–9183.

(24) Buch, I.; Giorgino, T.; De Fabritiis, G. Complete reconstruction of an enzyme-inhibitor binding process by molecular dynamics simulations. *Proc. Natl. Acad. Sci. U.S.A.* **2011**, DOI: 10.1073/pnas.1103547108.

(25) Jorgensen, W. L. Efficient Drug Lead Discovery and Optimization. *Acc. Chem. Res.* **2009**, *42* (6), 724–733.

(26) Gabdoulline, R. R.; Wade, R. C. Simulation of the diffusional association of barnase and barstar. *Biophys. J.* **1997**, *72* (5), 1917–1929.
(27) Gabdoulline, R. R.; Wade, R. C. Brownian dynamics simulation of protein-protein diffusional encounter. *Methods* **1998**, *14* (3), 329–41.
(28) Donald, L. E.; McCammon, J. A. Brownian dynamics with hydrodynamic interactions. *J. Chem. Phys.* **1978**, *69* (4), 1352–1360.
(29) García de la Torre, J.; Huertas, M. L.; Carrasco, B. Calculation of Hydrodynamic Properties of Globular Proteins from Their Atomic-Level Structure. *Biophys. J.* **2000**, *78* (2), 719–730.
(30) Dastidar, S. G.; Lane, D. P.; Verma, C. S. Modulation of p53 binding to MDM2: computational studies reveal important roles of Tyr100. *BMC Bioinf.* **2009**, *10* (Suppl 15), S6.
(31) Im, W.; Beglov, D.; Roux, B. Continuum Solvation Model: computation of electrostatic forces from numerical solutions to the Poisson-Boltzmann equation. *Comput. Phys. Commun.* **1998**, *111* (1−3), 59–75.
(32) Coalson, R.; Beck, T. L. Numerical Methods for Solving Poisson and Poisson-Boltzmann Type Equations. In *Encyclopedia of Computational Chemistry*; von Rague Schleyer, P., Ed.; John-Wiley: New York, 1998; Vol. 3, pp 2086−2100.
(33) Baker, N. A.; Sept, D.; Joseph, S.; Holst, M. J.; McCammon, J. A. Electrostatics of nanosystems: Application to microtubules and the ribosome. *Proc. Natl. Acad. Sci. U.S.A.* **2001**, *98* (18), 10037–10041.
(34) Dolinsky, T. J.; Czodrowski, P.; Li, H.; Nielsen, J. E.; Jensen, J. H.; Klebe, G.; Baker, N. A. PDB2PQR: expanding and upgrading automated preparation of biomolecular structures for molecular simulations. *Nucleic Acids Res.* **2007**, *35* (suppl 2), W522–W525.
(35) Czodrowski, P.; Dramburg, I.; Sotriffer, C. A.; Klebe, G. Development, validation, and application of adapted PEOE charges to estimate pKa values of functional groups in protein−ligand complexes. *Proteins: Struct., Funct., Bioinf.* **2006**, *65* (2), 424–437.
(36) Gabdoulline, R. R.; Wade, R. C. Protein-protein association: investigation of factors influencing association rates by Brownian dynamics simulations. *J. Mol. Biol.* **2001**, *306* (5), 1139–1155.
(37) Gabdoulline, R. R.; Wade, R. C. Effective Charges for Macromolecules in Solvent. *J. Phys. Chem.* **1996**, *100* (9), 3868–3878.
(38) Elcock, A. H.; Gabdoulline, R. R.; Wade, R. C.; McCammon, J. A. Computer simulation of protein-protein association kinetics: acetylcholinesterase-fasciculin. *J. Mol. Biol.* **1999**, *291* (1), 149–162.
(39) Hummer, G. Molecular binding: Under water's influence. *Nat. Chem.* **2010**, *2* (11), 906–7.
(40) Setny, P.; Baron, R.; McCammon, J. A. How Can Hydrophobic Association Be Enthalpy Driven?. *J. Chem. Theory Comput.* **2010**, *6* (9), 2866–2871.
(41) Seco, J.; Luque, F. J.; Barril, X. Binding site detection and druggability index from first principles. *J. Med. Chem.* **2009**, *52* (8), 2363–71.
(42) Brooks, C. L.; Onuchic, J. N.; Wales, D. J. Taking a Walk on a Landscape. *Science* **2001**, *293* (5530), 612–613.
(43) Huang, D.; Caflisch, A., The free energy landscape of small molecule unbinding. *PLoS Comput. Biol.* **2011**, *7* (2), e1002002.
(44) Conn, P. J.; Christopoulos, A.; Lindsley, C. W. Allosteric modulators of GPCRs: a novel approach for the treatment of CNS disorders. *Nat. Rev. Drug Discovery* **2009**, *8* (1), 41–54.
(45) Neckers, L.; Ivy, S. P. Heat shock protein 90. *Curr. Opin. Oncol.* **2003**, *15* (6), 419–24.
(46) Sharp, S. Y.; Prodromou, C.; Boxall, K.; Powers, M. V.; Holmes, J. L.; Box, G.; Matthews, T. P.; Cheung, K.-M. J.; Kalusa, A.; James, K.; Hayes, A.; Hardcastle, A.; Dymock, B.; Brough, P. A.; Barril, X.; Cansfield, J. E.; Wright, L.; Surgenor, A.; Foloppe, N.; Hubbard, R. E.; Aherne, W.; Pearl, L.; Jones, K.; McDonald, E.; Raynaud, F.; Eccles, S.; Drysdale, M.; Workman, P. Inhibition of the heat shock protein 90 molecular chaperone in vitro and in vivo by novel, synthetic, potent resorcinylic pyrazole/isoxazole amide analogues. *Mol. Cancer Ther.* **2007**, *6* (4), 1198−1211.
(47) Coe, D.; Armer, R.; Ratcliffe, A. Medicines research: current trends and case histories. Highlights of the Society for Medicines Research Symposium. *Drugs Future* **2009**, *34* (3), 247–254.
(48) Moll, U. M.; Petrenko, O. The MDM2-p53 Interaction. *Mol. Cancer Res.* **2003**, *1* (14), 1001–1008.
(49) Brown, C. J.; Cheok, C. F.; Verma, C. S.; Lane, D. P. Reactivation of p53: from peptides to small molecules. *Trends Pharmacol. Sci.* **2010**, *32* (1), 53–62.
(50) Lane, D. P.; Hupp, T. R. Drug discovery and p53. *Drug Discovery Today* **2003**, *8* (8), 347–355.
(51) Murray, J. K.; Gellman, S. H. Targeting protein-protein interactions: lessons from p53/MDM2. *Biopolymers* **2007**, *88* (5), 657–86.
(52) Joseph, T. L.; Madhumalar, A.; Brown, C. J.; Lane, D. P.; Verma, C. Differential binding of p53 and nutlin to MDM2 and MDMX: Computational studies. *Cell Cycle* **2010**, *9* (6), 1167–81.
(53) Walensky, L. D.; Kung, A. L.; Escher, I.; Malia, T. J.; Barbuto, S.; Wright, R. D.; Wagner, G.; Verdine, G. L.; Korsmeyer, S. J. Activation of Apoptosis in Vivo by a Hydrocarbon-Stapled BH3 Helix. *Science* **2004**, *305*, 1466–1470.
(54) Guo, Z.; Mohanty, U.; Noehre, J.; Sawyer, T. K.; Sherman, W.; Krilov, G. Probing the α-Helical Structural Stability of Stapled p53 Peptides: Molecular Dynamics Simulations and Analysis. *Chem. Biol. Drug Des.* **2010**, *75* (4), 348–359.
(55) Joseph, T. L.; Lane, D.; Verma, C. S. Stapled peptides in the p53 pathway: Computer simulations reveal novel interactions of the staples with the target protein. *Cell Cycle* **2010**, *9* (22), 4560–4568.
(56) Okazaki, K.-i.; Takada, S. Dynamic energy landscape view of coupled binding and protein conformational change: Induced-fit versus population-shift mechanisms. *Proc. Natl. Acad. Sci. U.S.A.* **2008**, *105* (32), 11182–11187.